JOURNAL OF Applied Polymer SCIENCE

Influence of temperature on the microstructure and mechanical properties of stretched polypropylene

Keran Li,[1] Bijin Xiong,[2] Ya Cao[1]

[1]State Key Laboratory of Polymer Materials Engineering, Polymer Research Institute of Sichuan University, Chengdu 610065, People's Republic of China

[2]Laboratoire MATEIS, INSA de Lyon, Bat. Blaise Pascal, 69621 Villeurbanne, France

Correspondence to: Y. Cao (E-mail: caoya@scu.edu.cn) and B. Xiong (E-mail: xiongbijin@hotmail.com)

ABSTRACT: Microstructure and mechanical properties of isotactic polypropylene (iPP) stretched at different temperatures were studied. Strain-induced fibrils were observed after stretching. Crystallinity (X_c), crystallite thickness (L_c), long period (L_{pf}), and diameter (D_f) of fibrils were characterized by Differential Scanning Calorimetry and Small angle X-ray scattering. L_{pf} of stretched iPP below 60°C was found to be lower than undrawn iPP. X_c, L_c, and D_f increased with increasing draw temperature. Tensile test showed that Young's moduli of stretched iPPs were negatively dependent on X_c and L_c. The fraction of taut tie molecules was estimated from the mechanical model. Results showed that more tie molecules were formed in the samples stretched at lower temperatures. Dynamical mechanical analysis showed that glass transition temperature was strongly dependent on the draw temperature. The glass transition peak disappeared in stretched iPPs obtained below 80°C. © 2015 Wiley Periodicals, Inc. J. Appl. Polym. Sci. **2015**, *132*, 42622.

KEYWORDS: mechanical properties; morphology; polyolefins; properties and characterization; structure-property relations

Received 25 April 2015; accepted 14 June 2015

DOI: 10.1002/app.42622

INTRODUCTION

Stretching with heat is one of the most effective manufacturing processes to modify the final properties of the products of semicrystalline polymers.[1–6] The morphology of the stretched products are strongly affected not only by the molecular topology but also by process conditions such as draw temperature, draw ratio, and the cooling rate after drawing.[2,7,8] In order to predict and optimize performance of the final drawing products, it is important to understand the structural deformation behavior during heat drawing of semicrystalline polymers.

Deformation of semicrystalline polymers involves structural change of polymers from a spherulites structure to an oriented fibrous structure at large strain. This is known as fibrillar transformation.[9–12] Two mechanisms of fibrillar transformation, fragmentation - reorganization of lamellar stacks and melting - recrystallization, were proposed in previous studies.[12–17] Firstly, the crystal blocks within the micro-fibrils of the deformed polyethylene mats were observed by TEM and Small angle X-ray scattering (SAXS).[13,16,18] The dimension of the crystalline blocks in the stretching direction was close to the thickness of the initial crystals. Based on these observations, the fibrillar transformation process was described as that the lamellae break into blocks and then the blocks rearrange into the micro-fibrils via chain unfolding from the fracture surface of the crystal blocks.[10] Secondly, long period of the micro-fibril (L_{pf}) formed by fibrilar transformation was different to the long period of original isotropic crystalline lamellae stacks (L_p), being 30% larger or 50% smaller than L_p.[9] For a given molecular topology, L_{pf} was found to be independent to the original microstructure but only dependent on the drawing conditions.[17,19] To explain the variation of long period, the original lamellae were supposed to be broken off by the local melting of blocks, and then the highly ordered melt recrystallized to form a new periodic structure.[14,20,21]

It is widely recognized that, when the semicrystalline polymers are drawn, the lamellar crystallites in the spherulites are more or less destroyed by shear forces depending on the temperature of drawing.[4] Decreasing of crystallinity after deformation has been observed because of destroy of the crystallites.[22] When semicrystalline polymer is hot drawn below the melting point, flow-induced crystallization could occur leading to increase of the crystallinity.[10,23] After hot drawing, polymers are highly fragmented and the *c*-axis is oriented in the stretching direction inducing very high strength in orientation direction.[12,24,25]

Deformation with a fibrillar transformation of semicrystalline polymers below the melting temperature was successful in developing very high stiffness and strength products.[26] This provided a way to improve the mechanical properties of polymers

without the addition of foreign reinforcements.[27,28] Ward *et al.*[29] obtained stretched iPP with an ultrahigh modulus of 19 GPa. Similarly, Kamezawa *et al.*[30] obtained the oriented iPP films with modulus of 15 GPa by cold draw. It was found that the higher draw ratio the higher modulus in the draw direction. Young's modulus of stretched iPP was found to be mainly governed by the fraction of taut tie molecules in amorphous phase.[31,32] The increase of modulus with increasing taut tie molecules was observed.[32] The fraction of taut tie molecule was dependent on temperature. It was loosened by annealing above 310 K, resulting in the shrinkage of the stretched film annealed at high temperature.[32] However, the role of the draw temperature on the fraction of taut tie molecule is not fully understood yet.

This article has two aims. First, a series of stretched polypropylenes were prepared by draw at different temperatures. Their microstructures were characterized to understand the influence of draw temperature on the fibrillar structure of polypropylene. The second aim is to investigate the mechanical properties of the stretched polypropylenes. The relationship between microstructure and properties of stretched polypropylene was studied.

EXPERIMENTAL

Materials

The iPP used in the experiments was a commercial product supplied by INEOS Company. The molecular weight M_w was 4.6×10^5 g/mol and the polydispersity $M_w/M_n = 3.3$. The iPP was used as received.

The iPP pellets were compression molded in a laboratory hot press at 220°C. The samples were completely melted for 10 min between two aluminum sheets prior to the application of a pressure of 10 MPa to produce iPP sheets. On removal from the press, the samples were quenched by plunged directly into cold water bath. The sheet was obtained with size of 10 cm × 10 cm × 500 μm. The quenched iPP was donated by PP-Q.

Stretched samples were prepared by draw of PP-Q at a constant strain rate of 1.39×10^{-3} s^{-1}, using a tensile machine MTS 1/ME, at draw temperature 50°C, 60°C, 70°C, 80°C, 90°C, 100°C, 110°C, and 120°C respectively. The rectangle-shaped specimens were cut from the quenched sheets with a cutter of 20 mm length and 10 mm width. The stretch process of PP-Q were stopped at draw ratio $\lambda = 4$. Then the stretched samples were cooled and relaxed at room temperature for 24 hours. The neck region of the stretched specimen was cut for the rest characterizations.

Differential Scanning Calorimetry

The measurement of crystallinity of iPP was carried out by an indium-calibrated Mettler DSC 7 instrument (Switzerland), using samples 5–7 mg. The controlled melting and cooling rates were maintained at 10°C/min, conducting under nitrogen flow 25 mL/min. The crystallinity, X_c, was estimated as follows:

$$X_c = \frac{\Delta H_m}{\Delta H_m^0} \quad (1)$$

where ΔH_m is the measured heat fusion and ΔH_m^0 is the heat fusion of a perfect crystal with 100% crystalline (207 J/g).[33] The standard deviation of the X_c data is about 1%.

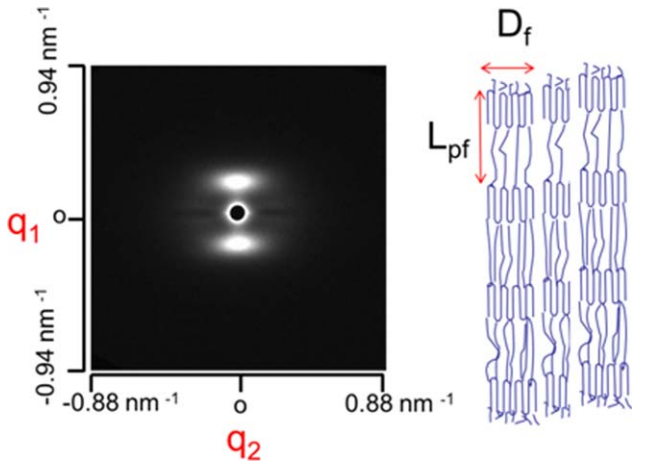

Figure 1. SAXS pattern of stretched iPP (draw temperature 60°C). The inset shows the geometry obtained from the SAXS patterns. [Color figure can be viewed in the online issue, which is available at wileyonlinelibrary.com.]

SAXS Measurement

SAXS experiments were performed on a laboratory X-ray diffract equipment using a wavelength $\lambda = 0.154$ nm. The 2D-SAXS patterns were recorded on a CCD camera (Ropper Scientific) which was set at 900 mm sample–detector distance.

The scattering pattern was recorded as shown in Figure 1. Fibril structure was observed after stretching as shown in the inset of Figure 1.[10,34] Structural data of micro-fibrils were estimated from the analysis of the one-dimensional intensity profile along the meridian and equatorial (see Figure 1). To calculate the long period of the fibrils, the intensity profiles along the meridian were obtained by projection of the 2D-patterns on the meridian according to Stribeck's method.[35] The long period of micro-fibril was estimated by equation:

$$L_{pf} = 2\pi/q_1^{max} \quad (2)$$

where q_1^{max} is the scattering vector at the maximum intensity profile of the correlation peak. The standard deviation of the L_{pf} does not exceed 1 nm

For the computation of the diameter of micro-fibrils, the scattering objects were supposed as the individual micro-fibrils embedded in a medium of lower electron density consisting of amorphous chains. The details of calculation method could be found elsewhere.[10] The equatorial contribution of the scattering factor could be performed via Guinier's approximation leading to an estimation of the equatorial size of the scattering element.[36–38] Guinier's approximation function of the equatorial intensity profile was[37]

$$I(q_2) = I_0 \exp\left(-\frac{q_2^2 D_f^2}{4}\right) \quad (3)$$

where D_f is the diameter of the scattering element. This equation is only valid for $qD_f << 1$. Thus Guinier's approximation only fitted at very low q_2 ($q_2 < 0.01$ nm^{-1}). The measured diameter of micro-fibrils (D_f) had a deviation of 0.5 nm.

The crystal thickness, L_c, was computed from the following relation:

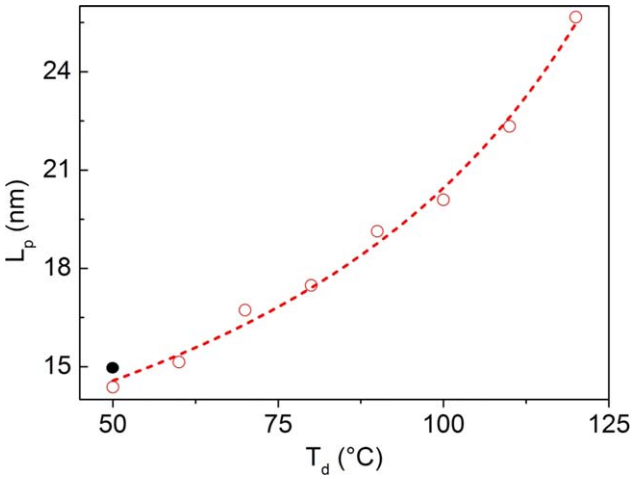

Figure 2. Long period of stretched iPP at draw temperatures range from 50°C to 120°C. Black solid circle represents the long period of undrawn sample. [Color figure can be viewed in the online issue, which is available at wileyonlinelibrary.com.]

$$L_c = L_p X_c \rho / \rho_c \quad (4)$$

$$\text{with} \quad \frac{1}{\rho} = \frac{X_c}{\rho_c} + \frac{1 - X_c}{\rho_a}$$

where L_p is long period, ρ_c is the density of the crystalline phase (0.95 g/cm^3)[39] and ρ_a is the density of amorphous phase (0.85 g/cm^3).[39]

Tensile Test

Tensile tests were performed by using a tensile machine MTS 1/ME at a constant strain rate 1.39×10^{-3} s^{-1} at room temperature. Dumbbell-shaped specimens were used for these tests. They were cut from the stretched sheets of 200 μm thickness by a cutter with the length direction in the pre-drawn direction. They had a gauge length of 6 mm and a width of 3 mm.

Dynamic Mechanical Analysis

Small pieces were cut in the different sheets to obtain parallelepipeds with a section about 5×0.5 mm^2 and a length between jaws about 14 mm. Experiments were conducted with an lab-made inverse torsion pendulum. The details of the experiments can be found elsewhere.[40] Measurements were performed at 1 Hz from 230 to 450 K at temperature scanning rate of 1 K/min. The storage modulus G', the loss modulus G'' and the loss factor tan δ were obtained.

RESULTS

Microstructures

The quenched iPP (*PP-Q*) used as starting material for stretch had a long period of 15 nm, the crystallinity of 0.49 and crystallite thickness of 5 nm. It should be mentioned that the stretch was stopped at draw ratio $\lambda = 4$ at which the strain hardening was not appearing at this point. This avoided the stretch of neck region after strain hardening.

The stretched sample yielded a two-spot meridional diffraction pattern as shown in Figure 1, suggesting a uniform orientation of stretched sample. Fibrillar structure was observed after stretching as shown in the inset of Figure 1.[10,34] The long period of stretched iPP (L_{pf}) were collected in Figure 2. As shown in Figure 2, a conspicuous influence of draw temperature (T_d) on L_{pf} can be observed. L_{pf} strongly increases with increasing T_d. Stretch above 60°C yields an increase of the long period; whereas stretch below 60°C causes a decrease of long period compared to the long period of undrawn iPP. It is can also be seen that T_d above 90°C results in a more abrupt increase. Similar results were obtained in case of the hot draw of polyethylene by Corneliussen and Peterlin.[20] This provides evidence that the firbillar transformation is not a feature limited to PE, but also has a more general significance to other semicrystalline polymer.

The relation between L_{pf} and T_d can be described as[13]

$$L_{pf} = A + \frac{B}{T_m - T_d} \quad (5)$$

where T_m is the melting temperature and T_d is the draw temperature, A and B are constants. By fitting the data of Figure 2, parameters A, B, and T_m were got to be 4.9, 1263.8, and 182.6, respectively. T_m is close to the equilibrium temperature of

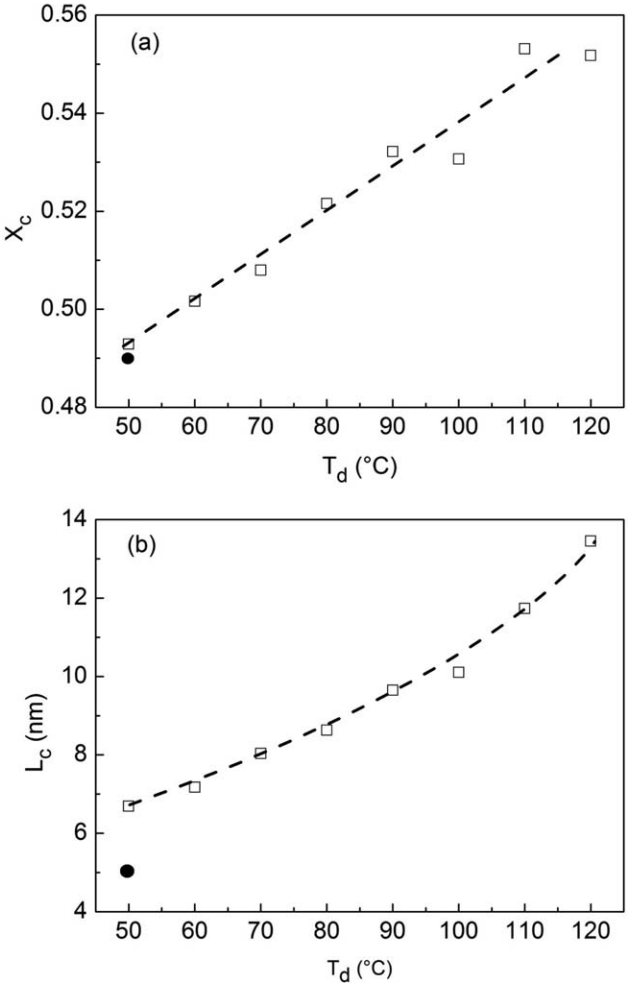

Figure 3. (a) Crystallinity of stretched iPP versus draw temperature ; (b) crystallite thickness of stretched iPP versus draw temperature. Black solid circles represent the crystallinity and crystallite thickness of undrawn sample.

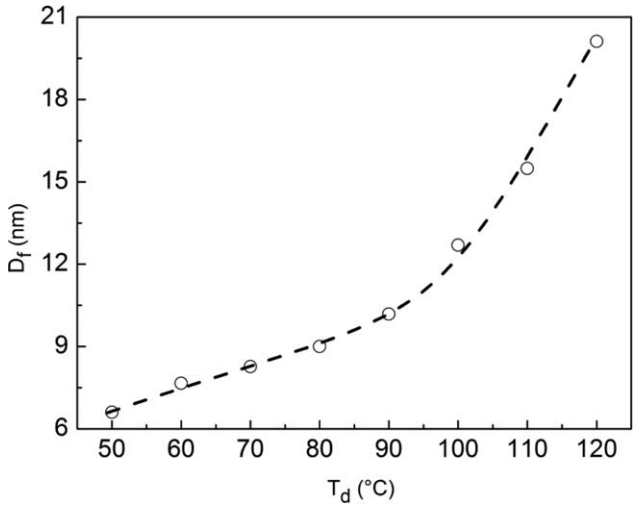

Figure 4. Diameter of micro-fibrils of stretched iPP in function of draw temperature.

186.2°C reported in the previous study.[41] This suggests that the stretched iPPs have relatively perfect crystal structures.

Figure 3 shows the crystallinity (X_c) and crystallite thickness (L_c) of stretched iPPs in function of T_d. X_c increases with increasing T_d as shown in Figure 3(a). At low T_d, a more abrupt increase can be observed. As shown in Figure 3(b), L_c also increases with increasing T_d. But a more abrupt increase of L_c appears at high temperature.

The diameters of the micro-fibrils, D_f, were estimated and collected in Figure 4. An increase of the D_f with the elevation of T_d can be observed. Below 90°C, well close to the α transition temperature (T_α) of PP-Q, D_f linearly increases with elevating temperature. Above 90°C, D_f presents more abrupt dependent on T_d. Humbert *et al.*[10] pointed out that D_f is mainly controlled by the fragmentation process of the initial crystal lamellae. It was found that D_f associates to the content of interphase which is generally assigned to the gathering all kinds of topological defects arising from the crystallization, i.e. chain entanglements, anchoring of tie molecules on the crystal, irregular chain-folds, chain ends, etc. The initial crystal lamellae are more likely to fragment from defect point, determine the size of the crystal of the micro-fibrils, because of the local stress concentration round the defects. Hedesiu *et al.*[42] found that the semi-rigid fraction of polypropylene, between crystal and amorphous phase, decreased with increasing temperatures. Hence draw at higher temperature, higher D_f appears because of the decrease of semi-rigid fraction. On the other hand, above T_α, taut tie molecule is relaxed because of the activation of chain mobility in crystal, preventing the local stress concentration in the anchoring of tie molecules. This could lead to the increase of the distance between two fragmentation points, further result in the increase of D_f with increasing T_d.

Mechanical Properties

Figure 5 shows the true stress–strain curves of pre-stretched iPP at room temperature. It should be mentioned that the sample was drawn in the pre-stretched direction and no necking and

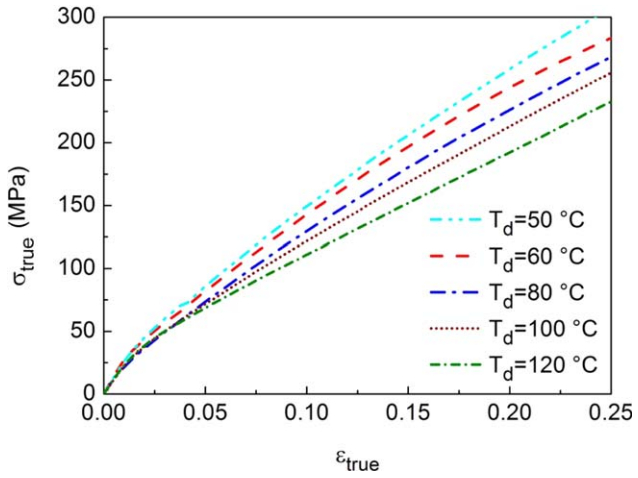

Figure 5. True stress–strain curves of stretched iPP in the drawing direction at room temperature. Strain rate 1.39×10^{-3} s^{-1}. [Color figure can be viewed in the online issue, which is available at wileyonlinelibrary.com.]

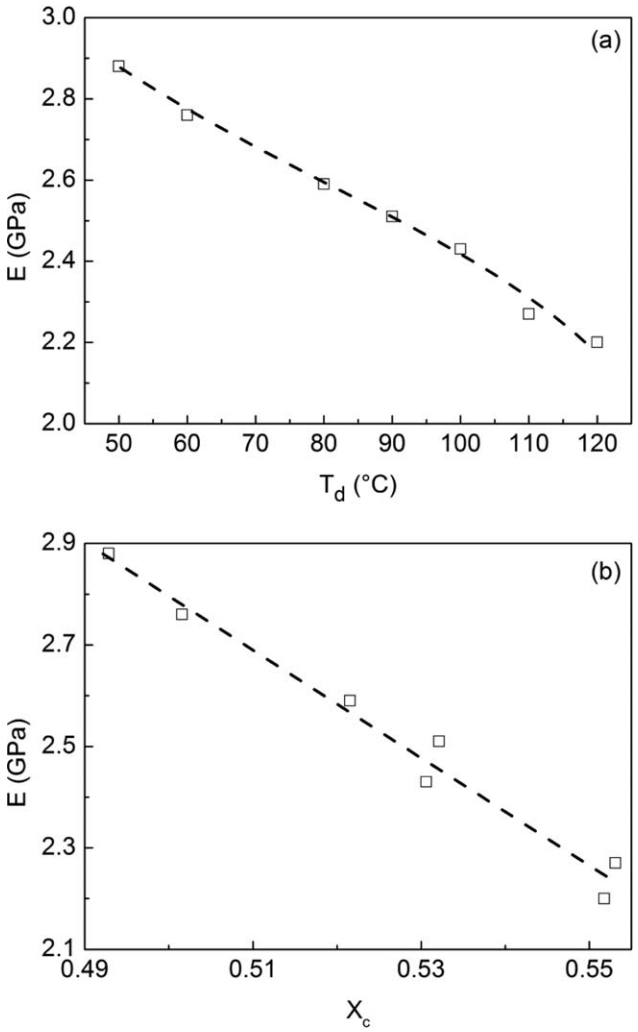

Figure 6. Young's modulus of stretched iPP versus (a) draw temperature and (b) crystallinity.

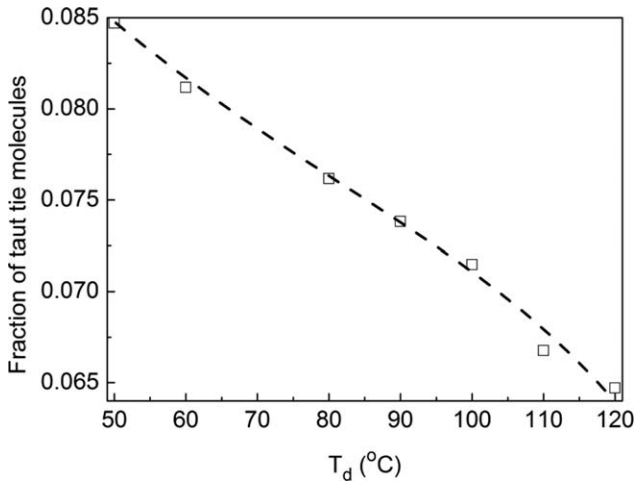

Figure 7. Fraction of taut tie molecules for stretched samples in function of draw temperature.

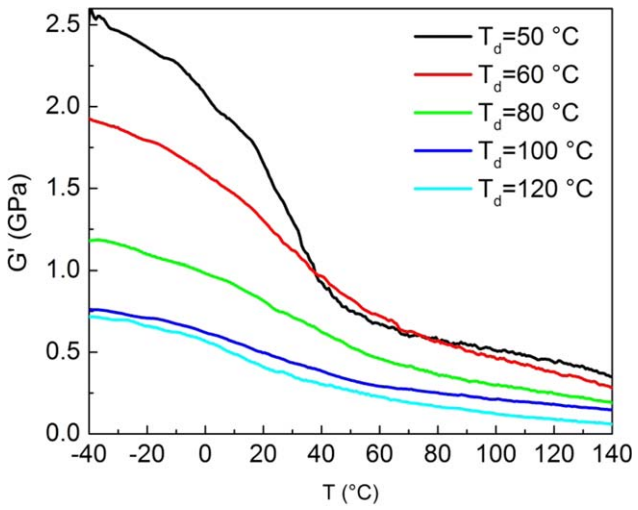

Figure 8. Variation of storage shear modulus, *G'*, of stretched samples with temperature measured at frequency 1 Hz and temperature scanning rate 1°C/min. [Color figure can be viewed in the online issue, which is available at wileyonlinelibrary.com.]

strain whitening were observed over the entire deformation. The yield occurs fast after a very small deformation, c.a. 0.02; and then a significant degree of strain hardening appears. The large positive slopes following yield can be observed. This is because of the fact that the stress is applied parallel to the normal of the lamellar structure and the crystallites cannot be skewed strongly.[43]

Young's moduli read from the tensile curves are plotted against the T_d and X_c in Figure 6. It can be seen that Young's modulus (E) decreases with increasing X_c and T_d. This behavior conflicts with the observation of isotropic iPP that the modulus positively depends on X_c.[44] This coincides to the observation of Nagou *et al.*[31] that the drawn iPP with higher crystallinity had a lower dynamic modulus along the draw direction.

The fraction of taut tie molecules was evaluated by using the composite model composed of the series and parallel connection of crystalline region and amorphous region according the previous studies.[30,32] The fraction of taut tie molecules could be written as the ratio of E/E_c, where E was Young's modulus in draw direction and E_c was the crystal modulus along the molecular axis which was 34 GPa. Figure 7 shows the fraction of taut tie molecules of stretched iPPs in function of T_d. As shown in Figure 7, the fraction of taut tie molecules decreases with increasing T_d. This could be because of the relaxation of taut tie molecule at high temperature.

Dynamical Mechanical Properties

Figure 8 shows the variation of storage shear modulus, *G'*, of stretched samples with temperature measured at frequency 1 Hz. The temperature scanning rate was 1°C/min. As shown in the graph, *G'* of stretched samples clearly decrease with increasing temperature as expected. The iPP stretched at the lower T_d shows the higher *G'*. This is similar to the variations of E observed in the tensile test. At 140°C, all the stretched samples possess similar *G'*, suggesting that the stretched samples are relaxed.

Figure 9 shows the variation of loss factor (tan δ) of stretched samples with temperature. Experiments conducted with frequency 1 Hz and temperature scanning rate 1°C/min. The undrawn sample shows a peak at ca. 0°C. This is associated to the glass transition temperature, T_g, of iPP. It is difficult to define the exact value of T_g from the graph since the peak is rather broad. Although the peak is weak, this peak can be observed in the specimens stretched above 80°C. The height of the peak is reduced with decreasing T_d. This could be because of the formation of the taut tie molecules in amorphous phase. For the samples stretched at low temperature, highly oriented amorphous chains were formed. If the amorphous phase becomes highly oriented, small segmental motions is difficult to occur because of the less freedom. The highly oriented chains of taut tie molecules require great thermal energy to active the conformational changes. Therefore, the magnitude of glass

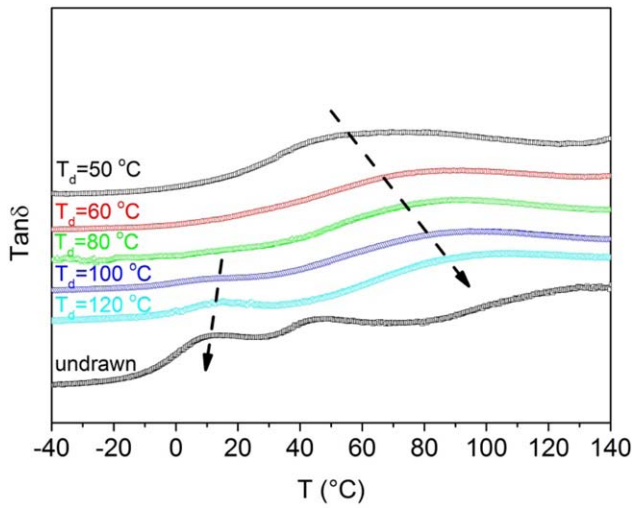

Figure 9. Loss factors of stretched iPPs and isotropic iPP plot in function of temperature measured at frequency 1 Hz and temperature scanning rate 1°C/min. [Color figure can be viewed in the online issue, which is available at wileyonlinelibrary.com.]

transition peaks seen in undrawn sample is greatly reduced or even disappear after stretching.

Figure 9 shows a broader peak in tan δ curves at higher temperature than T_g, which associates to the α transition. The temperature of α transition, T_α, increases with increasing T_d. This could be assigned to the increase of the L_c with increasing T_d. T_α dedicates the onset of segmental motion within the crystalline regions. The greater crystal continuity and greater crystalline stem length require greater thermal energy to allow conformational changes in crystal. This results in a higher temperature required for the α transition onset.

DISCUSSION

Crystallinity increase appears after the stretch of iPP. This suggests that crystallization process occurred in the tensile deformation. Humbert[10] also found that the crystallinity of drawn polyethylene at room temperature has higher value than quenched specimen. It was interpreted that the melt and recrystallization occur owing to the self-heating effect in the neck shoulder where a great amount of plastic work was locally transformed into heat. Further, the long period of stretched iPP is smaller than the original samples below 60°C. The discontinuous change of the long period suggests that destruction and reconstruction processes occur during the tensile deformation. These provide evidences to the melting-recrystallization mechanism for the fibrillar transformation.

Indeed the local temperature in the neck shoulder of cold-drawn iPP at room temperature had been observed to be higher than 50°C in the surface by an IR-radiation thermometer.[45] This proves that the self-heating does exist in the plastic deformation of iPP. Considering the thickness of the samples, the local temperature could be much higher inside the neck shoulder than in the surface. However, it should be pointed out that the "melt" in the neck might be very different from normal thermal melting. Because of the slow strain rate used in the tensile test, the temperature of the neck should be very close to room temperature. In such case the heating has enough time to dissipate, hence local temperature slightly increased. On the other hand, the applied mechanical energy might weaken van der Waals bonds between chains in polymer crystals and enhance the potential energy of the system during tensile test.[46,47] Chain randomization might occur at the draw temperature when the internal energy reached a critical value.

Negative dependence of Young's moduli on crystallinity was observed in stretched iPPs. However, Young's moduli increase with increasing the fraction of taut tie molecules. This suggests that Young's modulus of stretched iPP is mainly governed by the amorphous chains. Yamada *et al.*[1] had successfully correlated the orientation function of amorphous chains to Young's modulus. Although crystallinity of stretched iPP increases with increasing T_d, its low fraction of taut tie molecules dominates the modulus decrease with increasing T_d. The taut tie molecules are highly oriented between crystalline lamellae, so they are less freedom to engage in small segmental motions. In this case, the glass transition could not be observed by the dynamic mechanical analysis. These taut tie molecules can significantly enhance the mechanical properties in orientation direction. Young's modulus of isotropic PP crystallized with nucleation is in the range of 0.9–2 GPa[48] but in this study, Young's modulus is in the range of 2.1–2.9 GPa, higher than those of isotropic PPs.

CONCLUSION

Microstructure and mechanical properties of stretched iPPs by drawing at different temperatures were studied. Strain-induced fibrils were observed after stretching and their microstructures were characterized by SAXS and Differential Scanning Calorimetry. The microstructure of the stretched iPP is strongly influenced by draw temperature. The crystallinity (X_c), crystallite thickness (L_c), and long period (L_{pf}) of the micro-fibrils increase with increasing draw temperature. X_c and L_c of stretched samples are higher than those of undrawn sample. These provide evidences to the mechanism of melting and recrystallization for the fibrillar transformation during the deformation of polypropylene. The fraction of taut tie molecules of stretched iPPs decreases with increasing draw temperature.

Young's modulus is mainly dominated by the taut tie molecules in amorphous phase. Young's modulus of stretched iPPs negatively depends on the X_c and L_c. This is mainly because of the decrease of the fraction of taut tie molecules with increasing draw temperature. Dynamic mechanical analysis gets similar results. The iPP stretched at the lower T_d shows the higher storage modulus. The glass transition temperature is strongly dependent on the draw temperature. The magnitude of glass transition peaks seen in undrawn sample is greatly reduced or even disappear after stretching.

REFERENCES

1. Karger-Kocsis, J. Polypropylene Structure, Blends and Composites: Springer Science & Business Media, **1995**.
2. Ran, S.; Zong, X.; Fang, D.; Hsiao, B. S.; Chu, B.; Phillips, R. A. *Macromolecules* **2001**, *34*, 2569.
3. Samuels, R. J. *J. Polym. Sci. A* **1965**, *3*, 1741.
4. Sakurai, T.; Nozue, Y.; Kasahara, T.; Mizunuma, K.; Yamaguchi, N.; Tashiro, K.; Amemiya, Y. *Polymer* **2005**, *46*, 8846.
5. Cansfield, D.; Capaccio, G.; Ward, I. *Polym. Eng. Sci.* **1976**, *16*, 721.
6. Bigg, D. *Polym. Eng. Sci.* **1988**, *28*, 830.
7. Brown, N.; Ward, I. M. *J. Mater. Sci.* **1983**, *18*, 1405.
8. Fujiyama, M.; Kitajima, Y.; Inata, H. *J. Appl. Polym. Sci.* **2002**, *84*, 2128.
9. Peterlin, A. *Kolloid-Zeitschrift und Zeitschrift für Polymere* **1969**, *233*, 857.
10. Humbert, S.; Lame, O.; Chenal, J. -M.; Seguela, R.; Vigier, G. *Eur. Polym. J.* **2012**, *48*, 1093.
11. Peterlin, A. *J. Polym. Sci. C* **1967**, *18*, 123.
12. Peterlin, A. *J. Mater. Sci.* **1971**, *6*, 490.
13. Balta-Calleja, F.; Peterlin, A. *J. Macromol. Sci. B* **1970**, *4*, 519.

14. Jiang, Z. Y.; Tang, Y. J.; Rieger, J.; Enderle, H. F.; Lilge, D.; Roth, S. V.; Gehrke, R.; Heckmann, W.; Men, Y. F. *Macromolecules* **2010**, *43*, 4727.
15. Wang, H. P.; Chum, S. P.; Hiltner, A.; Baer, E. *J. Polym. Sci. B Polym. Phys.* **2009**, *47*, 1313.
16. Peterlin, A.; Corneliussen, R. *J. Polym. Sci. A-2 Polym. Phys.* **1968**, *6*, 1273.
17. Peterlin, A. *Colloid Polym. Sci.* **1987**, *265*, 357.
18. Sakaoku, K.; Peterlin, A. *J. Polym. Sci. A-2 Polym. Phys.* **1971**, *9*, 895.
19. Peterlin, A. *Polym. Eng. Sci.* **1969**, *9*, 172.
20. Corneliussen, R.; Peterlin, A. *Die Makromol. Chem.* **1967**, *105*, 193.
21. Butler, M. F.; Donald, A. M.; Ryan, A. J. *Polymer* **1998**, *39*, 39.
22. Pluta, M.; Bartczak, Z.; Galeski, A. *Polymer* **2000**, *41*, 2271.
23. Zuo, F.; Keum, J. K.; Chen, X.; Hsiao, B. S.; Chen, H.; Lai, S. -Y.; Wevers, R.; Li, J. *Polymer* **2007**, *48*, 6867.
24. Sadler, D.; Barham, P. *Polymer* **1990**, *31*, 36.
25. Nozue, Y.; Shinohara, Y.; Ogawa, Y.; Sakurai, T.; Hori, H.; Kasahara, T.; Yamaguchi, N.; Yagi, N.; Amemiya, Y. *Macromolecules* **2007**, *40*, 2036.
26. Nitta, K. -H.; Nomura, H. *Polymer* **2014**, *55*, 6614.
27. El-Maaty, M. A.; Bassett, D.; Olley, R.; Hine, P.; Ward, I. *J. Mater. Sci.* **1996**, *31*, 1157.
28. Hine, P.; Ward, M.; Teckoe, J. *J. Mater. Sci.* **1998**, *33*, 2725.
29. Cansfield, D. L. M.; Capaccio, G.; Ward, I. M. *Polym. Eng. Sci.* **1976**, *16*, 721.
30. Kamezawa, M.; Yamada, K.; Takayanagi, M. *J. Appl. Polym. Sci.* **1979**, *24*, 1227.
31. Nagou, S.; Azuma, K. *J. Macromol. Sci. B* **1979**, *16*, 435.
32. Yamada, K.; Kamezawa, M.; Takayanagi, M. *J. Appl. Polym. Sci.* **1981**, *26*, 49.
33. Wunderlich, B. Macromolecular Physics; Elsevier: Amsterdam, **2012**.
34. Bonart, R.; Hosemann, R. *Kolloid-Zeitschrift und Zeitschrift für Polymere* **1962**, *186*, 16.
35. Stribeck, N. Analysis of SAXS fiber patterns by means of projections. ACS Symposium Series, Vol. 739, ACS Publications: Washington, DC, **2000**, p 41.
36. Hasegawa, H.; Hashimoto, T.; Kawai, H.; Lodge, T. P.; Amis, E. J.; Glinka, C. J.; Han, C. C. *Macromolecules* **1985**, *18*, 67.
37. Guinier, A.; Fournet, G.; Walker, C. B.; Yudowitch, K. L. Small Angle Scattering of X-Rays; Wiley: New York, **1955**.
38. Humbert, S.; Lame, O.; Chenal, J. M.; Seguela, R.; Vigier, G. *Eur. Polym. J.* **2012**, *48*, 1093.
39. De Rosa, C.; Auriemma, F.; Corradini, P.; Tarallo, O.; Dello Iacono, S.; Ciaccia, E.; Resconi, L. *J. Am. Chem. Soc.* **2006**, *128*, 80.
40. Humbert, S.; Lame, O.; Séguéla, R.; Vigier, G. *Polymer* **2011**, *52*, 4899.
41. Yamada, K.; Hikosaka, M.; Toda, A.; Yamazaki, S.; Tagashira, K. *Macromolecules* **2003**, *36*, 4790.
42. Hedesiu, C.; Demco, D.; Kleppinger, R.; Poel, G. V.; Gijsbers, W.; Blümich, B.; Remerie, K.; Litvinov, V. *Macromolecules* **2007**, *40*, 3977.
43. Haward, R. *Macromolecules* **1993**, *26*, 5860.
44. Haward, R.; Thackray, G. *Proc. R. Soc. Lond. A* **1968**, *302*, 453.
45. Springer, H.; Schenk, W.; Hinrichsen, G. *Colloid Polym. Sci.* **1983**, *261*, 9.
46. Juska, T.; Harrison, I. R. *Polym. Eng. Sci.* **1982**, *22*, 766.
47. Li, J.; Cheung, W. *Polymer* **1998**, *39*, 6935.
48. Pukánszky, B.; Mudra, I.; Staniek, P. *J. Vinyl Addit. Technol.* **1997**, *3*, 53.